

Manganese(II)–Superoxide Complex in Aqueous Solution

Frank Jacobsen, Jerzy Holcman, and Knud Sehested*

Environmental Science and Technology Department, Risø National Laboratory, DK-4000 Roskilde, Denmark

Received: September 19, 1996; In Final Form: December 6, 1996[Ⓢ]

Mn(II)_{aq}–superoxide complex, MnO₂⁺, was formed in pulse radiolysis by three distinct routes: Mn(I) + O₂, Mn(II) + O₂⁻ and Mn(III) + H₂O₂. The stability of this complex was found to be governed by the two equilibria: Mn²⁺ + O₂⁻ ⇌ MnO₂⁺ (1,-1) and Mn²⁺ + HO₂ ⇌ MnO₂⁺ + H⁺ (6,-6). Both forward and reverse rate constants of the reactions involved in these equilibria were determined: $k_1 = (1.5 \pm 0.2) \times 10^8 \text{ M}^{-1} \text{ s}^{-1}$, $k_{-1} = (6.5 \pm 1.0) \times 10^3 \text{ s}^{-1}$; $k_6 = (1.1 \pm 0.2) \times 10^6 \text{ M}^{-1} \text{ s}^{-1}$, $k_{-6} = (6.5 \pm 1.0) \times 10^6 \text{ M}^{-1} \text{ s}^{-1}$, yielding $K_{1,-1} = (2.3 \pm 0.5) \times 10^4 \text{ M}^{-1}$ and $K_{6,-6} = 0.17 \pm 0.06$. The metal–oxy complex MnO₂⁺ decays by self-reaction with $k(\text{MnO}_2^+ + \text{MnO}_2^+) = (6.0 \pm 1.0) \times 10^6 \text{ M}^{-1} \text{ s}^{-1}$ and in acid solutions also by reaction with HO₂, $k(\text{MnO}_2^+ + \text{HO}_2) = (1.0 \pm 0.3) \times 10^7 \text{ M}^{-1} \text{ s}^{-1}$. In both cases stoichiometric amounts of H₂O₂ are formed as the end product. Mn(I) was formed by reduction of Mn²⁺ with H atoms. It has an absorption spectra with maxima at 290 and 340 nm with $\epsilon_{290} = 1300 \pm 200 \text{ M}^{-1} \text{ cm}^{-1}$ and $\epsilon_{340} = 1000 \pm 150 \text{ M}^{-1} \text{ cm}^{-1}$. It reacts with oxygen with $k(\text{Mn(I)} + \text{O}_2) = (6.0 \pm 1.0) \times 10^6 \text{ M}^{-1} \text{ s}^{-1}$. Mn(III) reacts with hydrogen peroxide with $k(\text{Mn(III)} + \text{H}_2\text{O}_2) = (2.8 \pm 0.3) \times 10^3 \text{ M}^{-1} \text{ s}^{-1}$.

Introduction

Reaction of manganese(II) complexes with O₂⁻/HO₂ radicals has been subject to numerous investigations to elucidate formation of the MnO₂⁺ complexes, their role in oxidation of Mn²⁺ to Mn³⁺, and the dismutation of superoxide.^{1,2} Most studies were performed with Mn²⁺ complexed by ligands such as formate, sulfate, phosphate, and pyrophosphate, while no information is available on the reactions of O₂⁻/HO₂ radicals with Mn²⁺–aquo ion. Studying the reaction of Mn(III) with H₂O₂ (ref 3), we realized that the chemistry of the Mn(II)_{aq}/superoxide plays an important role in this system. It also may have an impact on modeling of the oxidative power of the atmospheric aqueous phase as well as aqueous ozonation processes where manganese is used as a catalyst. This paper deals with a pulse radiolysis study of the formation and decay and acid–base properties of the MnO₂⁺–aquo complex.

Experimental Section

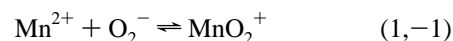
The 10 MeV Linac at Risø (Haimson Research Corp., HRC-712) providing pulses of 0.2–4 μs duration and a detection system consisting of a 450 W xenon lamp, quartz cell (light path: 5.1 cm), Perkin Elmer double quartz prism monochromator and photomultiplier IP28 (ref 4) equipped with a LeCroy (Model 9400) storage oscilloscope, and an IBM PC/AT3 computer on line for data processing were used. For the experiments where hydrogen gas was used to scavenge OH radicals the high-pressure cell⁵ with a light path length of 2.5 cm was used. Prior to pulse radiolysis the solutions were equilibrated 20–30 min with H₂ or a H₂/O₂ mixture at the desired pressure.

A hexacyanoferrate(II) dosimeter, $G = 5.9$, $\epsilon_{420} = 1000 \text{ M}^{-1} \text{ cm}^{-1}$, was used for determination of the absorbed dose. Manganous perchlorate hexahydrate purum p.a. from Fluka and MnSO₄ monohydrate Analar from BDH were used as received. Gases were of N40 quality, and all other chemicals were of p.a. quality. All solutions were freshly prepared from triply distilled water.

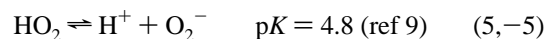
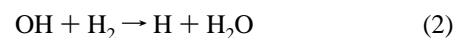
Hydrogen peroxide formed in pulse radiolysis was determined spectrophotometrically as FeSO₄⁺ at 305 nm in 0.4 M H₂SO₄.⁶ Modeling of the experimental results was carried out using the CHEMSIMUL^{7,8} program for the numerical simulation of chemical systems.

Results and Discussion

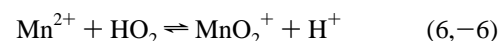
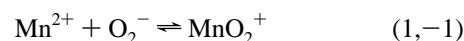
Reaction of Mn²⁺ with O₂⁻/HO₂ Radicals. When formate, sulfate, phosphate, or pyrophosphate is used as a ligand for complexing Mn²⁺, the metal–oxy complex MnO₂⁺ is formed in the reversible reaction with superoxide:^{1,2}



To avoid use of formate as an OH-scavenger, solutions containing Mn(ClO₄)₂ were equilibrated with 140 atm H₂ and 2–3 atm O₂ to convert the OH radicals into hydroperoxy radicals. In this system all primary radicals are converted into O₂⁻/HO₂ radicals according to



The radicals O₂⁻/HO₂ were found to react with Mn²⁺ with a pH-dependent rate to form an absorption with a maximum at 270 nm (Figure 1).



We ascribe this spectrum to the aquo metal–oxy complex MnO₂⁺ on the basis of its similarity to the spectra of MnO₂⁺ species obtained with Mn(II)–formate, –sulfate, –phosphate, or –pyrophosphate complexes.^{1,2} As the shape of the observed

[Ⓢ] Abstract published in *Advance ACS Abstracts*, January 15, 1997.

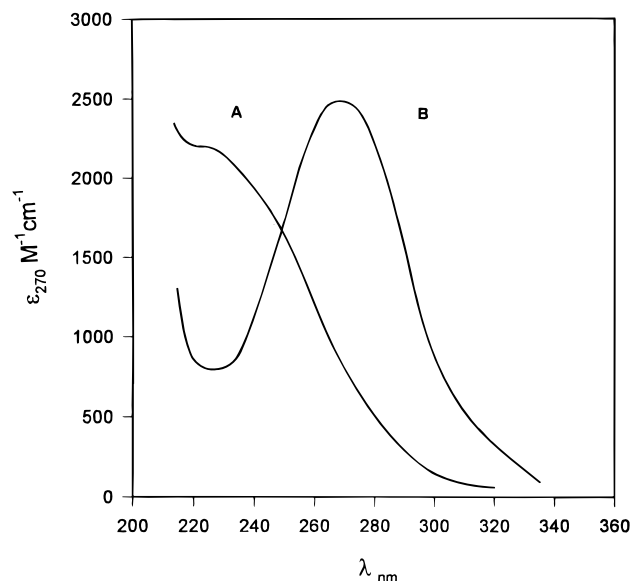


Figure 1. Absorption spectra of (A) HO_2/O_2^- radicals obtained 2.3 μs after a 1.0 μs , 2.0 krad pulse and (B) MnO_2^+ -aquo complex measured 50 μs after a 1.0 μs , 2.0 krad pulse. Both obtained with $[\text{Mn}^{2+}] = 2.0 \times 10^{-3} \text{ M}$, 3.0 atm O_2 , 140.0 atm H_2 , at pH 5.5.

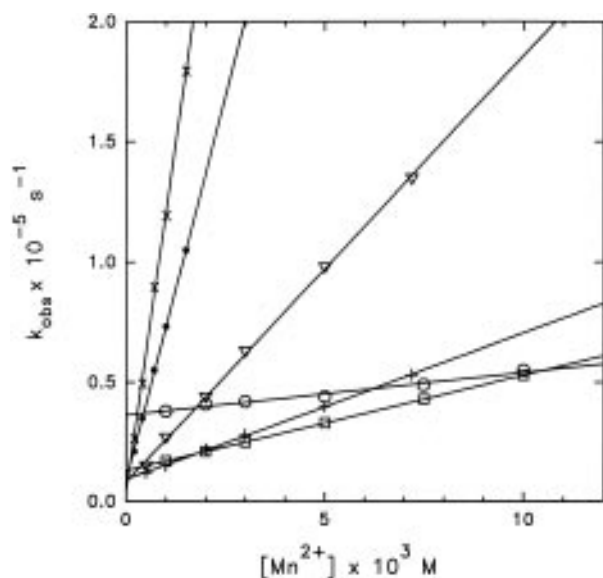


Figure 2. Apparent first-order rate constant k_{obs} for the buildup of MnO_2^+ measured at 270 nm as a function of $[\text{Mn}^{2+}]$: (○) pH 2.4, (□) pH 3.0, (+) pH 3.4, (▽) pH 4.0, (●) pH 4.8, and (×) pH 5.5 (1 krad, 22 °C, and ionic strength $\mu = (3.2\text{--}3.5) \times 10^{-2} \text{ M NaClO}_4$).

spectrum does not change with pH, we choose to interpret reaction 6 as a formation of the same complex and a proton rather than formation of the protonated metal-oxo complex.

Extrapolating $1/[\text{Mn}^{2+}]$ in solutions at pH 5–6 to zero, an extinction coefficient of $\text{MnO}_2^+(\text{aq}) \epsilon_{270} = 2500 \pm 300 \text{ M}^{-1} \text{ cm}^{-1}$ was obtained, comparable with the extinction coefficients reported for the Mn(II) complexes.^{1,2}

The rate constants of the equilibrium reactions (1,–1) and (6,–6) were determined by pulse radiolysis of solutions equilibrated with 140 atm H_2 and 3 atm O_2 by varying pH (2.0–6.0) and the $\text{Mn}(\text{ClO}_4)_2$ concentration. All experiments were performed at constant ionic strengths of $(3.2\text{--}3.5) \times 10^{-2} \text{ M}$ adjusted with NaClO_4 and with a 1 μs pulse of 1 krad. The formation of the MnO_2^+ complex was followed as a first-order buildup at 270 nm. At the higher pH range (pH 4–6) the slope of the plot of k_{obs} vs $[\text{Mn}^{2+}]$, Figure 2, increases with pH due to the difference between the rate constants k_1 and k_6 and in

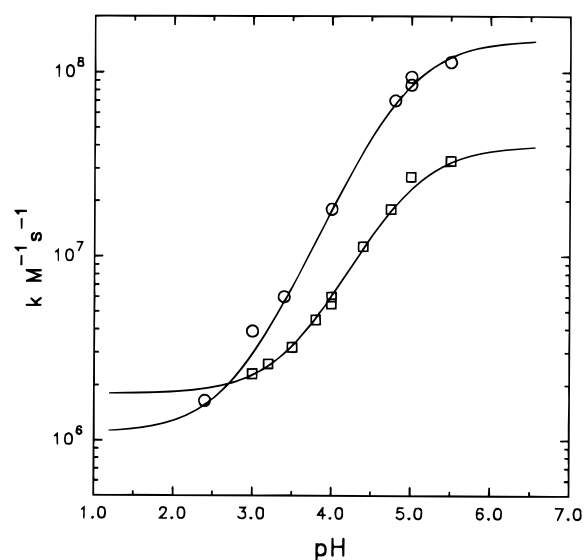


Figure 3. Second-order rate constant $k(\text{Mn}^{2+} + \text{HO}_2/\text{O}_2^-)$, calculated from the slopes of k_{obs} vs $[\text{Mn}^{2+}]$ in Figure 2, as a function of pH: (○) HClO_4 and (□) H_2SO_4 at 22 °C. Solid curves calculated for $\text{p}K_a = 4.9$ for the HO_2/O_2^- couple, $k_1 = 1.5 \times 10^8$, $k_6 = 1.1 \times 10^6 \text{ M}^{-1} \text{ s}^{-1}$ for HClO_4 and $k'_1 = 4.0 \times 10^7$, $k'_6 = 1.8 \times 10^6 \text{ M}^{-1} \text{ s}^{-1}$ for H_2SO_4 , respectively (1 krad, 22 °C, and ionic strength $\mu = (3.2\text{--}3.5) \times 10^{-2} \text{ M NaClO}_4$).

accordance with the ratio $[\text{O}_2^-]/[\text{HO}_2]$ given by the equilibrium (5,–5), while the intercept remains constant, yielding $k_{-1} = (6.5 \pm 1.0) \times 10^3 \text{ s}^{-1}$. In the lower pH range (pH 2–4) the slope of the plot of k_{obs} vs $[\text{Mn}^{2+}]$ still increases with increasing pH, but the intercept appears to be an increasing function of $[\text{H}^+]$. This behavior is in accordance with the mechanism based on the equilibria (5,–5), (1,–1), and (6,–6). The influence of $[\text{H}^+]$ on the intercept is first observed when the value of $k_{-6} \times [\text{H}^+]$ becomes comparable to k_{-1} .

The spectra were measured for each experimental condition, and although the yield at 270 nm decreases with increasing $[\text{H}^+]$ and increases with Mn^{2+} concentration, the observed spectrum could always be accounted for as a composite of the three species MnO_2^+ , O_2^- , and HO_2 . As neither the kinetics nor the spectra indicate the presence of a protonated form of the complex, $\text{MnO}_2\text{H}^{2+}$, we do not include this species in our mechanism, although its presence has been suggested in the study of Mn(II) complexes.^{1,2}

At high $[\text{Mn}^{2+}]$ concentrations formation of a dimeric species $\text{MnO}_2\text{HMn}^{4+}$ has been suggested^{1,2} with an absorption spectrum identical to that of MnO_2^+ . We do not include this dimeric species into our mechanism, as the increase of absorption at 270 nm with increasing Mn^{2+} concentration at low pH (the main argument for introducing the $\text{MnO}_2\text{HMn}^{4+}$ species^{1,2}) can be qualitatively accounted for by equilibrium (6,–6). This conclusion is corroborated by the observation of a corresponding decrease of absorption at 220 nm.

The rate constants calculated from the slopes of k_{obs} vs $[\text{Mn}^{2+}]$ in Figure 2 are plotted as a function of pH, Figure 3. The solid lines in Figure 3 conform to the standard equation, derived for a rate constant of reaction of O_2^-/HO_2 radicals being in equilibrium with a species existing in only one form in this pH region.

$$k = \frac{k_6 + k_1(K_5/[\text{H}^+])}{1 + (K_5/[\text{H}^+])} \quad (\text{I})$$

The best fit of eq I to the experimental points is obtained with $k_1 = (1.5 \pm 0.2) \times 10^8 \text{ M}^{-1} \text{ s}^{-1}$ and $k_6 = (1.1 \pm 0.2) \times 10^6$

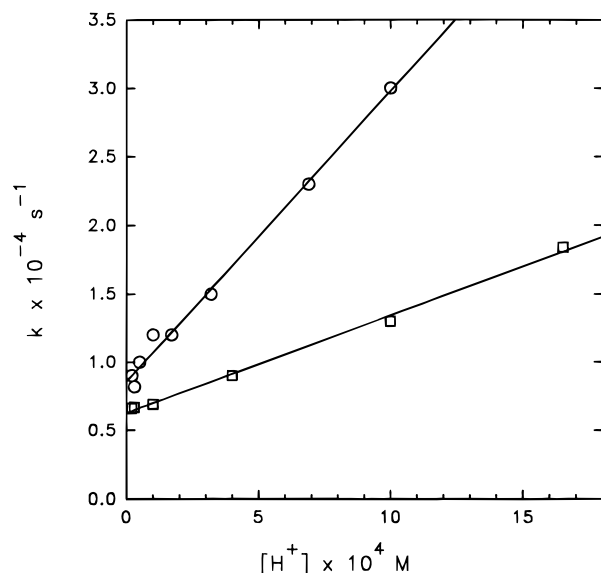


Figure 4. Intercepts of plots of k_{obs} vs $[\text{Mn}^{2+}]$ from Figure 2 as a function of H^+ concentration: (\square) HClO_4 and (\circ) H_2SO_4 (1 krad, 22 °C, and ionic strength $\mu = (3.2\text{--}3.5) \times 10^{-2}$ M NaClO_4).

$\text{M}^{-1} \text{s}^{-1}$. Unfortunately, the experimental determination of k_1 and k_6 at plateau regions of the curves in Figure 3 is not feasible, as it requires extremely high $\text{Mn}(\text{II})$ concentrations at the low-pH end, while at the high-pH end it is hindered by hydrolysis of $\text{Mn}(\text{II})$. With $k_{-1} = (6.5 \pm 1.0) \times 10^3 \text{ s}^{-1}$ determined from the intercepts in Figure 2 an equilibrium constant $K_{1,-1} = (2.3 \pm 0.5) \times 10^4 \text{ M}^{-1}$ is derived. The plot of the intercepts from Figure 2 vs the H^+ concentration in the lower pH range (Figure 4) yields $k_{-6} = (6.5 \pm 1.0) \times 10^6 \text{ M}^{-1} \text{ s}^{-1}$. The rate constants k_6 and k_{-6} yield an equilibrium constant $K_{6,-6} = 0.17 \pm 0.06$. From the respective rate constants it follows that the presence of acid shifts the equilibrium toward free HO_2 radicals. Indeed below pH 2 with moderate concentrations of Mn^{2+} the only absorption observed was the spectrum of HO_2 decaying in second-order kinetics with the rate constant within the literature value $k = (8.3 \pm 0.7) \times 10^5 \text{ M}^{-1} \text{ s}^{-1}$ (ref 9).

For comparison the sulfate metal–oxy complex was also studied. The only difference from the system in refs 2 and 3 is that no formate was added as an OH-scavenger. In our system the OH radicals were converted into H atoms by H_2 and thereby to O_2^-/HO_2 radicals by the O_2 present (reactions 2–5). In solutions containing 0.1 M sulfate equilibrated with H_2 at 140 atm and O_2 at 3 atm the Mn^{2+} concentration was varied in the range 5.0×10^{-4} to 10^{-2} M and the pH was varied in the range 3.0–5.5.

Again the formation of the MnO_2^+ complex was followed as a first-order buildup of absorption at 270 nm. By a procedure analogous to that applied above for the aquo–ion the following rate constants for equilibria (1,–1) and (6,–6) in the sulfate system were obtained: $k'_1 = (4.0 \pm 0.5) \times 10^7 \text{ M}^{-1} \text{ s}^{-1}$, $k'_{-1} = (8.5 \pm 2.0) \times 10^3 \text{ s}^{-1}$, $k'_6 = (1.8 \pm 0.2) \times 10^6 \text{ M}^{-1} \text{ s}^{-1}$, and $k'_{-6} = (2.1 \pm 0.5) \times 10^7 \text{ M}^{-1} \text{ s}^{-1}$ (Figure 4). These rate constants allow an equilibrium constant for sulfate metal–oxy complex $K'_{1,-1} = (4.7 \pm 1.3) \times 10^3 \text{ M}^{-1}$, in good agreement with literature values, $(6.0 \pm 1.0) \times 10^3 \text{ M}^{-1}$ at 0.5 M sulfate and $(1.0 \pm 0.2) \times 10^4 \text{ M}^{-1}$ at 0.1 M sulfate (both obtained in the presence of formate).^{1,2} Furthermore $K'_{6,-6} = (8.6 \pm 2.3) \times 10^{-2}$ was derived. As was the case with the Mn^{2+} aquo–ion, the spectra obtained at low pH in all cases could be accounted for by the presence of only three species, MnO_2^+ , O_2^- , and HO_2 , distributed according to the equilibria (1,–1), (5,–5), and (6,–6). A different mechanism was put forward

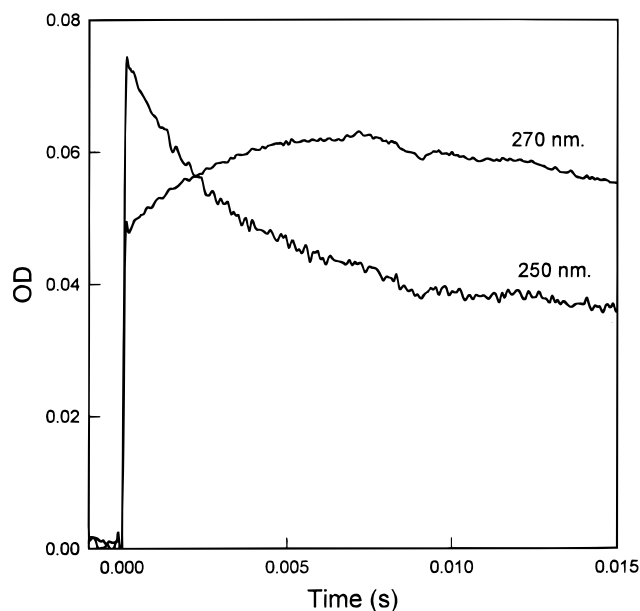
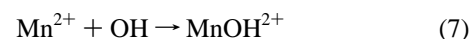


Figure 5. Absorption traces obtained in pulse radiolysis of 0.1 M Mn^{2+} at pH 3.5 (HClO_4), 3.0 atm O_2 , 5.0×10^{-3} M H_2O_2 , and dose 2.0 krad. Decay of Mn^{3+} at 250 nm and buildup of MnO_2^+ at 270 nm.

in the literature^{1,2} based on the formation of a MnOOH^{2+} species by addition of HO_2 to Mn^{2+} in an irreversible reaction. However, we were not able to observe any spectral or kinetic property that would distinguish the MnOOH^{2+} species from the HO_2 radical, and the irreversible formation of the MnOOH^{2+} violates the principle of microscopic reversibility and detailed balance (no virtual equilibrium for HO_2). Therefore we suggest that the mechanism consistent for the equilibria (1,–1), (5,–5), and (6,–6) is more plausible in the cases of the Mn^{2+} aquo–ion and sulfate complex.

Formation of MnO_2^+ in the Reaction $\text{Mn}(\text{III}) + \text{H}_2\text{O}_2$. $\text{Mn}(\text{III})$ was formed in the reaction of Mn^{2+} with OH radicals.



From a buildup of absorption at 220–250 nm at various $[\text{Mn}^{2+}]$ in the pH range 0–6 the rate constant $k_7 = (2.0 \pm 0.2) \times 10^7 \text{ M}^{-1} \text{ s}^{-1}$ was measured, which is somewhat lower than the literature values 3.6×10^7 and $2.9 \times 10^7 \text{ M}^{-1} \text{ s}^{-1}$ (ref 10) and $2.6 \times 10^7 \text{ M}^{-1} \text{ s}^{-1}$ (ref 11).

The absorption spectrum of $\text{Mn}(\text{III})$ at pH 0–3 has $\lambda_{\text{max}} = 220 \text{ nm}$ and $\epsilon(\text{MnOH}^{2+})_{220} \approx 5000 \text{ M}^{-1} \text{ cm}^{-1}$, while at 270 nm $\epsilon(\text{MnOH}^{2+})_{270} \approx 1000 \text{ M}^{-1} \text{ cm}^{-1}$ (refs 3, 10), less than half of that of the manganese–superoxide complex ($\epsilon(\text{MnO}_2^+)_{270} = 2500 \text{ M}^{-1} \text{ cm}^{-1}$).

By pulse radiolysis of N_2O -saturated 0.1 M $\text{Mn}(\text{ClO}_4)_2$ and 5.0×10^{-3} M H_2O_2 solution at pH 3.5 a first-order decay at 250 nm concomitant with a first-order buildup at 270 nm was observed, Figure 5. While the initial spectrum was that of MnOH^{2+} , the spectrum developed after 5–10 ms was that of MnO_2^+ . The spectrum measured after 1.5 ms in a solution of 5×10^{-2} M Mn^{2+} , 3.3×10^{-2} M H_2O_2 , and O_2 saturated at pH 3.0 irradiated with a 2 krad pulse matches exactly the spectrum obtained in pulse radiolysis of a 10^{-2} M Mn^{2+} solution at pH 3.0 equilibrated with 140 atm H_2 and 3 atm O_2 using the same 2 krad pulse (Figure 6). In the N_2O -saturated solutions about two-thirds of OH radicals react with Mn^{2+} (reaction 7) forming MnOH^{2+} and one third reacts with H_2O_2 forming HO_2 radicals. MnOH^{2+} and HO_2 radicals thus formed react with H_2O_2 (reaction 8) and Mn^{2+} (reaction 6) respectively, both yielding the MnO_2^+ complex. In the system under H_2 pressure

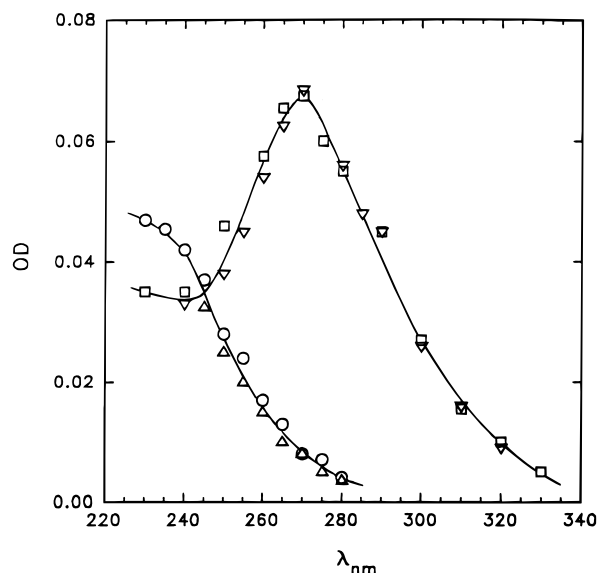
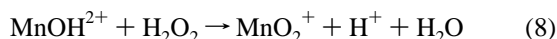


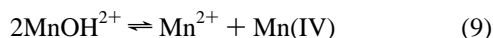
Figure 6. Absorption spectra obtained with a 2.0 krad pulse in HClO_4 at 22 °C: (∇) 5.0×10^{-2} M Mn^{2+} , 3.3×10^{-2} M H_2O_2 , 1.0 atm O_2 at pH 3.0 measured 1.5 ms after pulse; (\square) 1.0×10^{-2} M Mn^{2+} , 2.0 atm O_2 and 140 atm H_2 at pH 3.0 measured 50 μs after pulse; (\triangle) 5.0×10^{-2} M Mn^{2+} , 3.3×10^{-2} M H_2O_2 , 1.0 atm O_2 at pH 0 measured 3 ms after pulse; and (\circ) 5.0×10^{-3} M Mn^{2+} , 1.0 atm O_2 and 140 atm H_2 at pH 0 measured 50 μs after pulse.

all OH radicals react with hydrogen (reaction 2), and then H atoms react with oxygen (reaction 3) to form HO_2 radicals, which successively yield the MnO_2^+ complex by reaction with Mn^{2+} . As a result of equilibria (1,-1) and (6,-6) the MnO_2^+ complex dominates at pH 3 (>95%), while free HO_2 radicals are dominant at pH < 1 (Figure 6).

Taking into account the stoichiometry of the reaction between Mn(III) and H_2O_2 , $\Delta[\text{Mn(III)}]/\Delta[\text{H}_2\text{O}_2] = 2$ (ref 12), we conclude that the above experimental findings are best interpreted in terms of reaction 8.



The observed rate of reaction 8 was found to decrease slightly with the Mn^{2+} concentration and increase with pH. The reason for the $[\text{Mn}^{2+}]$ dependence is the formation of Mn(IV) species due to disproportionation of Mn(III) according to equilibrium 9 (refs 10, 13) and a fast reaction of the Mn(IV) species with hydrogen peroxide.³



Therefore, the rate constant for reaction 8 was obtained by extrapolating $1/[\text{Mn}^{2+}]$ to zero, that is, as the intercept of the plot of the initial first-order rate constant vs $1/[\text{Mn}^{2+}]$ in Figure 7. The rate constant thus obtained, $k_8 = (2.8 \pm 0.3) \times 10^3 \text{ M}^{-1} \text{ s}^{-1}$, is practically pH-independent in the pH range 0–2. The increase of k_8 observed at higher pH (Figure 8) is ascribed to the presence of Mn(OH)_2^+ , a different hydrolytic form of Mn(III).^{11,14}

The absorption spectra measured at various pH's at 1.5–3 ms after the pulse were in all cases a composite either of O_2^-/HO_2 and MnO_2^+ or below pH 1 only of the HO_2 radical (Figure 6). At pH < 1, under our experimental conditions, reverse reaction -6 shifts the metal-oxy complex formed in reaction 8 to Mn^{2+} and HO_2 radicals. The identity of the HO_2 is confirmed by identity of the spectra and the decay kinetics yielding $k = 1.0 \times 10^6 \text{ M}^{-1} \text{ s}^{-1}$, in good agreement with the literature value.⁹

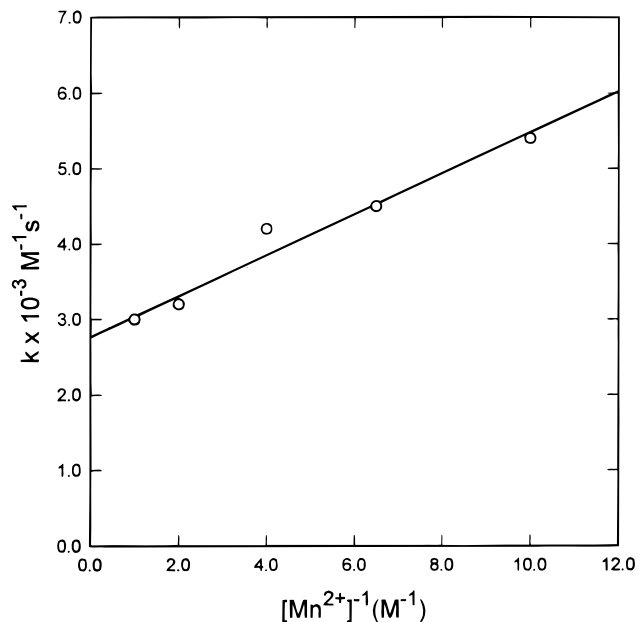


Figure 7. Rate constant of the $\text{Mn}^{3+} + \text{H}_2\text{O}_2$ reaction as a function of the reciprocal Mn^{2+} concentration (1 krad, 22 °C, in 1.0 M HClO_4).

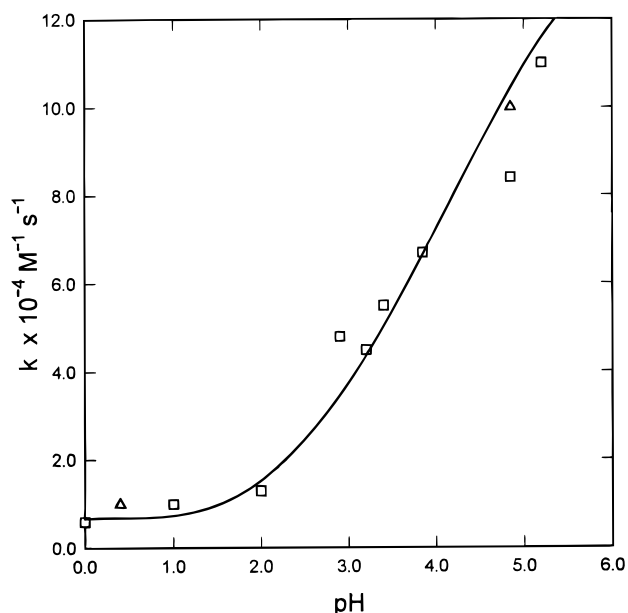
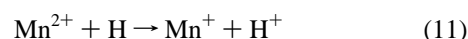
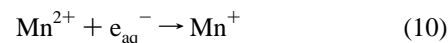


Figure 8. Apparent rate constant of $\text{Mn}^{3+} + \text{H}_2\text{O}_2$ as a function of pH in (\square) HClO_4 and (\triangle) H_2SO_4 solutions (1 krad, 22 °C, with $[\text{Mn}^{2+}] = 0.1 \text{ M}$).

Formation of MnO_2^+ in the Reaction $\text{Mn}^+ + \text{O}_2$. The hydrated electron and H atom are known to reduce Mn^{2+} to Mn^+ with rate constants $2.0 \times 10^7 \text{ M}^{-1} \text{ s}^{-1}$ (ref 15) and $6.6 \times 10^8 \text{ M}^{-1} \text{ s}^{-1}$ obtained in 6 M H_2SO_4 (ref 16), respectively.



The rate constant for reaction 11 in air-free 0.1 M perchloric acid equilibrated with 140 atm H_2 where both the hydrated electrons and OH radicals are converted into H atoms by H^+ and H_2 , respectively, $k_{11} = (2.0 \pm 0.2) \times 10^8 \text{ M}^{-1} \text{ s}^{-1}$, was measured in this study. The spectrum of Mn^+ (Figure 9), obtained under these conditions with $5 \times 10^{-3} \text{ M Mn}^{2+}$, exhibits two maxima at 290 and 340 nm with $\epsilon_{290} = 1300 \pm 200 \text{ M}^{-1} \text{ cm}^{-1}$ and $\epsilon_{340} = 1000 \pm 150 \text{ M}^{-1} \text{ cm}^{-1}$, respectively.

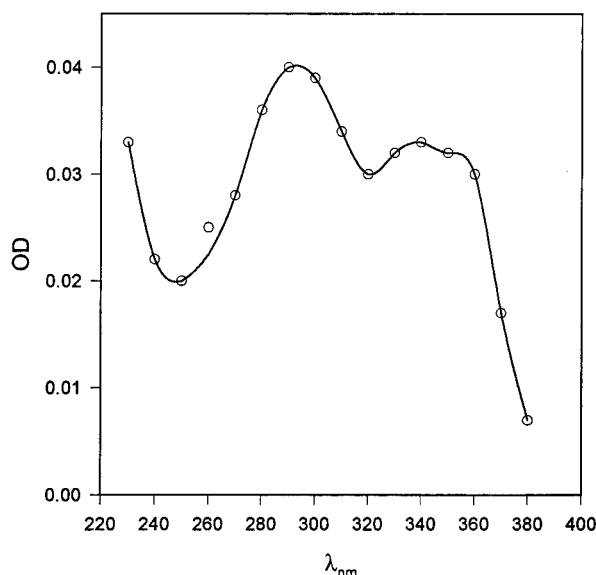
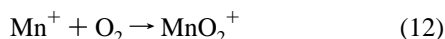


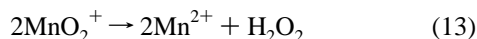
Figure 9. Spectrum of Mn^+ . Conditions: $[\text{Mn}^{2+}] = 1.0 \times 10^{-3}$ M, air-free solution of 0.1 M HClO_4 with 140 atm H_2 at 22 °C.

In an air-saturated 0.1 M Mn^{2+} solution at pH 3 equilibrated with 140 atm H_2 about two-thirds ($G \approx 4.2$) of the initial radicals form Mn^+ , the rest being divided between Mn(III) ($G \approx 1.0$) and HO_2 ($G \approx 1.3$). A first-order decay observed at 350 nm with an apparent rate constant proportional to the oxygen concentration is attributed to reaction 12:



Varying O_2 concentration within the range $(0.25\text{--}1.2) \times 10^{-3}$ M, a rate constant $k_{12} = (6.0 \pm 1.0) \times 10^6 \text{ M}^{-1} \text{ s}^{-1}$ was determined. Formation of the MnO_2^+ species is confirmed at higher pH by a concomitant buildup of the absorption spectrum with $\lambda_{\text{max}} = 270$ nm, while at pH < 1 only the HO_2 spectrum (a result of equilibrium (6,−6) with a small amount of the Mn(III) absorption (formed in reaction 7) is observed.

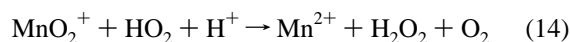
Decay of the MnO_2^+ Complex. In solutions close to neutral pH with 140 atm H_2 and 3 atm O_2 and high concentrations of Mn^{2+} and at fairly high doses (5–8 krad/pulse) MnO_2^+ decayed in second-order kinetics according to eq 13. A second-order rate constant $k_{13} = (6.0 \pm 1.0) \times 10^6 \text{ M}^{-1} \text{ s}^{-1}$ was determined.



Determination of H_2O_2 formed by single-pulse radiolysis showed stoichiometrical amounts of H_2O_2 , according to eq 13. On the basis of this result and experiments with H_2O_2 added, we can estimate the upper limit for the reaction $\text{MnO}_2^+ + \text{H}_2\text{O}_2$ to $k \leq 10^3 \text{ M}^{-1} \text{ s}^{-1}$.

On lowering the pH the decay became faster but still confirmed pretty well second-order kinetics. However, the observed decay is now governed by a cooperative action of the

equilibria (1,−1) and (6,−6) together with the cross reaction 14.



At even lower pH's (pH < 2) the decay kinetics turned into first-order as the excess of HO_2 radicals over MnO_2^+ increases with decreasing pH due to equilibrium (6,−6). Computer modeling of the MnO_2^+ decay yields the rate constant $k_{14} = (1.0 \pm 0.3) \times 10^7 \text{ M}^{-1} \text{ s}^{-1}$.

In all cases studied, the end product of the MnO_2^+ decay was H_2O_2 and Mn^{2+} . Neither with the aquo-ion nor with the sulfate complex could indications of the formation of binuclear species be observed. No formation of Mn(III) species could be detected during decay of MnO_2^+ neither in perchlorate nor in sulfate medium. This is reasonable having in mind that the MnO_2^+ is formed in reaction 8 with both the aquo-ion and sulfate complex and the difference of ca. 1.8 V in standard reduction potential between $\text{Mn}^{3+}/\text{Mn}^{2+}$ and O_2/O_2^- pairs. It seems that formation of Mn(III) in $\text{Mn(II)}/\text{O}_2^-$ requires the presence of ligands that can radically decrease the reduction potential of the $\text{Mn(III)}/\text{Mn(II)}$ pair.

Conclusion

The MnO_2^+ complex forms in the reaction of Mn(I) , Mn(II) , and Mn(III) with O_2 , O_2^-/HO_2 , and H_2O_2 , respectively. Interactions of O_2^-/HO_2 radicals with Mn^{2+} in the absence of complexing ligands or as the sulfate complex can be adequately described by the equilibria (1,−1), (5,−5), and (6,−6).

Acknowledgment. The authors wish to thank Torben Johansen for skillful operation of the linear accelerator. Financial support from the Commission of the European Communities within the Environment research program (Contract RINOXA EV5V-ct93-0317) is gratefully acknowledged.

References and Notes

- (1) Cabelli, D. E.; Bielski, B. H. J. *J. Phys. Chem.* **1984**, *88*, 3111.
- (2) Cabelli, D. E.; Bielski, B. H. J. *J. Phys. Chem.* **1984**, *88*, 6291.
- (3) Jacobsen F.; Holcman J.; Sehested K. To be published.
- (4) Sehested, K.; Holcman J. *J. Phys. Chem.* **1975**, *82*, 651.
- (5) Christensen, H.; Sehested, K. *Radiat. Phys. Chem.* **1980**, *16*, 183.
- (6) Sehested, K.; Rasmussen O. L.; Fricke H. *J. Phys. Chem.* **1968**, *72*, 626.
- (7) Bjergbakke, E.; Rasmussen, O. L.; Sehested, K.; Christensen, H. *RISØ-M-2430*, Risø National Laboratory, Roskilde, Denmark, 1984.
- (8) Rasmussen, O. L.; Bjergbakke, E. *RISØ-R-395*, Risø National Laboratory, Roskilde, Denmark 1984.
- (9) Bielski, B. H. J.; Cabelli, D. E.; Arudi, R. L.; Ross, A. B. *J. Phys. Chem. Ref. Data* **1985**, *14*, 1044.
- (10) Pick-Kaplan, M.; Rabani, J. *J. Phys. Chem.* **1976**, *80*, 1840.
- (11) Baral, S.; Lume-Pereira, C.; Janata, E.; Henglein, A. *J. Phys. Chem.* **1986**, *90*, 6025.
- (12) Davies, G.; Kirschenbaum, L. J.; Kustin, K. *Inorg. Chem.* **1968**, *7*, 146.
- (13) Davies, G. *Coord. Chem. Rev.* **1969**, *4*, 199.
- (14) Bidermann, G.; Palombari, R. *Acta Chem. Scand. A* **1978**, *32*, 381.
- (15) Rabani, J.; Mulac, W. A.; Matheson, M. S. *J. Phys. Chem.* **1977**, *81*, 104.
- (16) Dainton, F. S.; Phillipson, N. A.; Pilling, M. J. *J. Chem. Soc., Faraday Trans. 1* **1975**, *71*, 2377.